Atmos. Chem. Phys., 14, 9279–9293, 2014
www.atmos-chem-phys.net/14/9279/2014/
doi:10.5194/acp-14-9279-2014

Atmospheric Chemistry and Physics
Open Access

Contributions of vehicular carbonaceous aerosols to $PM_{2.5}$ in a roadside environment in Hong Kong

X. H. H. Huang[1], Q. J. Bian[2,*], P. K. K. Louie[3], and J. Z. Yu[1,2]

[1]Institute for the Environment, Hong Kong University of Science & Technology, Clear Water Bay, Kowloon, Hong Kong
[2]Department of Chemistry, Hong Kong University of Science & Technology, Clear Water Bay, Kowloon, Hong Kong
[3]Hong Kong Environmental Protection Department, 47/F, Revenue Tower, 5 Gloucester Road, Wan Chai, Hong Kong
[*]now at: Department of Atmospheric Science, Colorado State University, USA

Correspondence to: J. Z. Yu (jian.yu@ust.hk)

Received: 21 November 2013 – Published in Atmos. Chem. Phys. Discuss.: 2 January 2014
Revised: 7 July 2014 – Accepted: 29 July 2014 – Published: 9 September 2014

Abstract. Hourly measurements of elemental carbon (EC) and organic carbon (OC) were made at Mong Kok, a roadside air quality monitoring station in Hong Kong, for a year, from May 2011 to April 2012. The monthly average EC concentrations were 3.8–4.9 $\mu g\,C\,m^{-3}$, accounting for 9.2–17.7 % of the $PM_{2.5}$ mass (21.5–49.7 $\mu g\,m^{-3}$). The EC concentrations showed little seasonal variation and peaked twice daily, coinciding with the traffic rush hours of a day. Strong correlations were found between EC and NO_x concentrations, especially during the rush hours in the morning, confirming vehicular emissions as the dominant source of EC at this site. The analysis by means of the minimum OC / EC ratio approach to determine the OC / EC ratio representative of primary vehicular emissions yields a value of 0.5 for $(OC/EC)_{vehicle}$. By applying the derived $(OC/EC)_{vehicle}$ ratio to the data set, the monthly average vehicle-related OC was estimated to account for 17–64 % of the measured OC throughout the year. Vehicle-related OC was also estimated using receptor modeling of a combined data set of hourly NO_x, OC, EC and volatile organic compounds characteristic of different types of vehicular emissions. The $OC_{vehicle}$ estimations by the two different approaches were in good agreement. When both EC and vehicle-derived organic matter (OM) (assuming an OM-to-OC ratio of 1.4) are considered, vehicular carbonaceous aerosols contributed $\sim 7.3\,\mu g\,m^{-3}$ to $PM_{2.5}$, accounting for ~ 20 % of $PM_{2.5}$ mass (38.3 $\mu g\,m^{-3}$) during winter, when Hong Kong received significant influence of air pollutants transported from outside, and ~ 30 % of $PM_{2.5}$ mass (28.2 $\mu g\,m^{-3}$) during summertime, when local emission sources were dominant. A reduction of 3.8 $\mu g\,m^{-3}$ in vehicular carbonaceous aerosols was estimated during 07:00–11:00 (i.e., rush hours on weekdays) on Sundays and public holidays. This could mainly be attributed to less on-road public transportation (e.g., diesel-powered buses) in comparison with non-holidays. These multiple lines of evidence confirm local vehicular emissions as an important source of $PM_{2.5}$ in an urban roadside environment and suggest the importance of vehicular emission control in reducing exposure to $PM_{2.5}$ in busy roadside environments.

1 Introduction

Carbonaceous species is an important constituent of $PM_{2.5}$ (atmospheric particulate matter with aerodynamic diameters less than 2.5 µm) (Seinfeld and Pandis, 1998) and a substantial contributor to climate forcing, visibility impairment and adverse health effects (e.g., USEPA, 2004; IPCC, 2007). The carbonaceous material is commonly distinguished in elemental carbon (EC) and organic carbon (OC). EC has an exclusive origin in primary emissions from combustion of carbonaceous matter such as diesel, gasoline, biomass and organic wastes. In particular, EC dominates the particle fraction of diesel engine exhaust, which has recently been reclassified as carcinogenic to humans (e.g., USEPA, 2002; IARC, 2012). EC has been considered to undergo little chemical transformation in the atmosphere, and thus it has been used as an indicator for primary combustion emissions. OC can be directly generated from primary emission sources (known as primary OC, POC) or formed through oxidation of reactive

organic gases followed by gas-to-particle conversion processes in the atmosphere (known as secondary OC, SOC) (Gelencsér, 2004).

A significant fraction of $PM_{2.5}$ mass, ranging from 16 % in rural areas to around 40 % in urban/roadside areas, was identified as carbonaceous aerosols in Hong Kong (DRI, 2010; HKUST, 2013). A clear regional–urban–street gradient from low to high in total carbon (TC) concentrations has been consistently observed within Hong Kong during the past decade. The higher EC concentrations at street level reflect the important contribution from traffic emissions. While there exist a few studies examining the relative contributions of vehicular emissions to the $PM_{2.5}$ mass and its organic fraction in Hong Kong, fewer efforts have been focused on roadside $PM_{2.5}$ sources. Zheng et al. (2006) analyzed filter samples collected at three contrasting sampling sites with respect to vehicular emission influence during 2000–2001. They employed a chemical mass balance receptor model in combination with organic tracers to apportion contribution of nine air pollution sources to $PM_{2.5}$ OC. The contributions to OC from vehicular emissions were reported to be approximately 70 % at the roadside site, 60 % at the urban site and 25 % at the rural site. Guo et al. (2009) applied principal component analysis with absolute principal component scores technique to the $PM_{2.5}$ composition data obtained from two 1-year studies in Hong Kong and showed that vehicle emissions contributed about 51, 23 and 20 % to the $PM_{2.5}$ mass at the roadside, urban site and rural site, respectively. Hu et al. (2010) analyzed high-volume $PM_{2.5}$ samples collected at four sites during the summer of 2006 and used positive matrix factorization and chemical mass balance models to apportion the source contributions to OC. The results showed that vehicular exhaust contributed 41.0 and 8.4 % to the ambient OC on sampling days that were mainly under the influence of local emissions and regional transport, respectively. These source analysis studies were all based on 24 h filter measurements and they are inherently incapable of capturing the dynamics of pollutant emissions and atmospheric chemical conversion processes that happen on a faster time scale.

The Hong Kong Government has recognized the street-level air pollution as one of the most important air pollution issues for Hong Kong and has taken a wide range of measures to control the vehicular emissions (HKEPD, 2013). Hence, continuous efforts are in urgent need to monitor $PM_{2.5}$ components closely related to vehicular emissions and to estimate their contributions to $PM_{2.5}$ mass for the purpose of evaluating and formulating control measures targeting lowering the roadside $PM_{2.5}$.

In this study, a semicontinuous thermal–optical carbon field analyzer was deployed at Mong Kok (MK), one of the three roadside air quality monitoring stations (AQMS) in Hong Kong. Mong Kok, with its extremely high population density of 130 000 persons per square kilometer, is described as the busiest district in the world by the Guinness World Records. Measurements of hourly OC and EC concentrations were conducted for a year from May 2011 to April 2012. These high-time-resolution OC and EC data were analyzed to examine their diurnal, weekly, monthly and seasonal variations. The objectives are to derive the OC / EC ratio representing primary vehicular emissions and to estimate the contributions of vehicular carbonaceous aerosols to $PM_{2.5}$ in the roadside environment in Hong Kong.

2 Experimental

2.1 Sampling equipment and method

A semicontinuous OC–EC field analyzer system (RT-3131, Sunset Laboratory, OR, USA) was installed at the MK AQMS, a roadside site located in a mixed residential and commercial district in Hong Kong with heavy traffic and surrounded by many tall buildings. At the MK AQMS, a few aerosol samplers are located on a platform around 3 m above ground level, and instruments for the criteria gas pollutants are housed in a room at the site with their inlets extending through the ceiling. The OC–EC analyzer used in this work was located on the ground with the inlet ~ 2 m above the ground and ambient air was drawn through a 2.5 µm aerodynamic diameter cut-point cyclone at a flow rate of 8 L min^{-1}. A carbon-impregnated parallel plate organic denuder is placed upstream of the analyzer for removing gaseous organics. The analyzer was programmed to collect particle samples for 46 min at the start of each hour, followed by a 9 min sample analysis and 3 min instrument-stabilizing process.

The thermal–optical analytical method is based on the modified National Institute for Occupational Safety and Health (NIOSH) method 5040 protocol (Turpin et al., 1990; Birch and Cary, 1996; NIOSH, 2003). During the thermal analysis, the sample deposited on the quartz fiber filter is heated under different conditions and carbonaceous materials in the sample are converted to CO_2 for detection by the nondispersive infrared (NDIR) detector. In the first stage, thermal ramping occurs in a helium (He) environment from room temperature to 840 °C to volatize OC, followed by a brief cooling step to 550 °C. In the second stage, the carrier gas is switched to oxygen in helium (O_2 / He) and the temperature is increased stepwise to 870 °C, oxidizing off all of the EC in the sample. The temperature profiles and purge gases in each analysis stage is presented in Table S1 in the Supplement. Since a fraction of the OC could be pyrolyzed under the O_2-free conditions, a tuned diode laser (660 nm) is used to monitor the light transmission during the thermal analysis. In a typical analysis, the laser transmittance signals first decreases due to the pyrolysis of OC, and then increases as the pyrolyzed OC is oxidized in the presence of O_2. When the laser signal returns to its initial value at the beginning of the analysis, this sets the split point differentiating OC and EC.

Ultrahigh-purity grade gases (He, 10 % O_2 in He and 5 % CH_4 in He) were used. An O_2 trap (SGT Middelburg V. V., the Netherlands) was installed in the He gas line to remove trace amounts of O_2. The quartz fiber filters were prebaked inside the main oven of the instrument at 870 °C for about 5 min before sample collection and were replaced weekly.

In addition, hourly data including $PM_{2.5}$ mass, NO, NO_2 and O_3 at the sampling site are provided by the Hong Kong Environmental Protection Department (HKEPD).

2.2 Quality control and data validation

The semicontinuous carbon analyzer collected samples approximately 90 % of the time between 1 May 2011 and 30 April 2012. No data were collected during 21 June–20 July 2011 due to instrument maintenance and during 23–30 August 2011 due to malfunctioning of the NDIR detector.

The analyzer computer was closely monitored through a secured phone line, and the instrument was checked daily for any error flags for hardware or software problems. Weekly routine instrument maintenance includes sample filter replacement, cyclone cleaning, one-point external calibration, and checking of gas flow and instrument blanks. The instrument blank for total carbon (TC) during the study period ranged from 0.02 to 0.25 µgC, with an average of 0.13 µgC. For the 1 h measurement (46 min sampling at a flow rate of 8 L min^{-1}), the blank values translate to 0.05–0.66 µg C m^{-3} (average of 0.35 µg C m^{-3}) in atmospheric concentrations. The method detection limits (MDLs), determined to be 3 times the blank standard deviation, were 0.60 µg C m^{-3} for OC and 0.20 µg C m^{-3} for EC. Multi-point external calibrations using known sucrose concentrations spiked on a prebaked filter were conducted once every 1–2 months. As recommended by the manufacturer, 21.03 µgC was used for one-point calibration, while 4.21, 21.03 and 42.07 µgC were used for multi-point calibration. The recoveries of these three sucrose standard solutions were 119.0 ± 8.4, 100.7 ± 6.0 and 95.3 ± 7.1 %, respectively. When the organic denuder was changed once every 2 months, the sampling flow rate calibration was performed and the actual flow rates were recorded within 8.0 ± 0.4 L min^{-1}. Several experiments were conducted to determine the dynamic blank by placing a 47 mm Teflon filter upstream of the denuder and sampling particle-free ambient air into the analyzer on a 2 h collection/analysis cycle. The dynamic blank was in the range of 0.46–0.83 µg C m^{-3}, with an average of 0.68 µg C m^{-3}. The average dynamic blank corresponds to 8.7 % of the measured annual mean OC value. This value is consistent with the results from previous studies (e.g., Polidori et al., 2006; Kang et al., 2010) and the finding from Turpin et al. (1994) that the adsorption artifact is dependent on the concentrations of gaseous OC/particulate OC. The volatilization of particulate OC from the sampling quartz fiber filter was estimated to be 10 ± 6 % (upper limit) (Polidori et al., 2006). Considering that the positive and negative artifacts are of comparable magnitude, no correction was made to the measured OC concentrations in this study. The results from the dynamic blank test serve as an estimate of adsorption effect.

The data validation processes include checking of sampling volume, calibration peak area, NDIR signals and OC–EC split point. Data with a sampled volume variation beyond the tolerance of 5 % (i.e., 368 ± 18 L) or a calibration peak area variation beyond the tolerance of 10 % were considered to be invalid and excluded from the data set. The raw data files of all the collected samples were manually inspected to identify any abnormal OC–EC split (i.e., the time when the laser signal returns to its initial value after the pyrolysis). In the case of abnormal split, the calculation software of the instrument was then used to process the raw data files with the split point set manually. The data valid rate for the entire sampling period is 96 %. The effective sampling duration, data capture rates and valid rates for individual month are listed in Table S2 in the Supplement.

The semicontinuous OC and EC measurements (also abbreviated as RT measurements for ease of discussion) were further validated by comparing with OC and EC data obtained from two sets of offline filter-based measurements. One is from the Hong Kong $PM_{2.5}$ speciation network program. In the speciation monitoring program, $PM_{2.5}$ samples were collected on prebaked 47 mm quartz fiber filters over a 24 h (starting from 00:00) period by a Partisol sampler (Rupprecht & Patashnick, model 2025, NY, USA). The 24 h filter-based measurements using the Partisol samplers, abbreviated as Partisol-TC, Partisol-OC and Partisol-EC hereafter, were made every sixth day throughout the year. The other one is from the $PM_{2.5}$ organic speciation project. $PM_{2.5}$ samples were collected on prebaked 20 cm × 25 cm quartz fiber filters over a 24 h (starting from 00:00) period by a high-volume (HV) $PM_{2.5}$ particulate sampler (Tisch Environmental Inc., OH, USA) at a frequency of once every 3 days. The HV sampler-derived measurements are abbreviated as HV-TC, HV-OC and HV-EC hereafter. The sampled filters from both projects were stored in a freezer below −20 °C after collection and were analyzed using a lab-based thermal–optical carbon analyzer (Sunset Laboratory, OR, USA). The ACE-Asia protocol (Schauer et al., 2003), a variant of the NIOSH protocol (Wu et al., 2012), was used for these 24 h filter samples. The hourly OC and EC concentrations were averaged over the same 24 h period for comparison with the filter-based concentrations. The comparisons are shown in Fig. 1.

The differences between the measurements were evaluated by zero-intercept linear regression, average percent relative bias (%$\overline{RB}$) and average percent relative standard deviation (%$\overline{RSD}$). The equations to calculate these two parameters are given in Appendix 1 in the Supplement. The instrument blanks for both the bench-top aerosol carbon analyzer and the field OC-EC analyzer were statistically not different from zero after considering the analytical and instrumental uncertainties of the blank. Hence, the zero-intercept linear regression analysis was applied in the comparisons of the data sets.

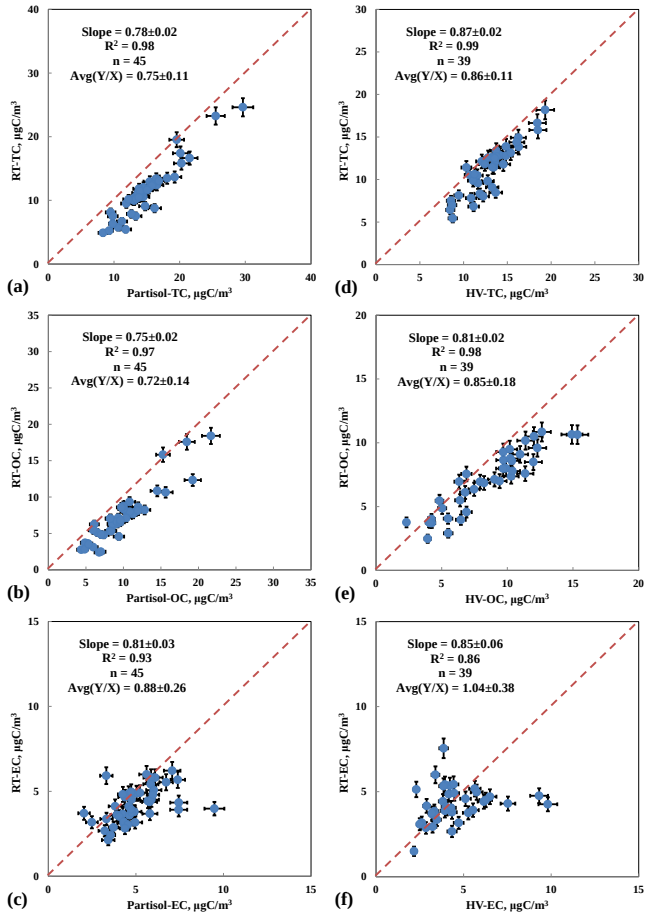

Figure 1. Scatter plots of semicontinuous measurements versus filter-based chemical data for $PM_{2.5}$ samples collected at MK AQMS during May 2011–April 2012. **(a)** RT-TC vs. Partisol-TC by thermal–optical transmittance (TOT) method, **(b)** RT-OC vs. Partisol-OC by TOT, **(c)** RT-EC vs. Partisol-EC by TOT, **(d)** RT-TC vs. HV-TC by TOT, **(e)** RT-OC vs. HV-OC by TOT and **(f)** RT-EC vs. HV-EC by TOT.

TC derived by means of the semicontinuous method agrees reasonably well with both Partisol filter measurements ($R^2 = 0.98$, $\%\overline{RB} = -29.6\,\%$, $\%\overline{RSD} = 23.4\,\%$) and HV filter measurements ($R^2 = 0.99$, $\%\overline{RB} = -16.4\,\%$, $\%\overline{RSD} = 15.2\,\%$). Good correlations and reasonable agreement were also observed for OC ($R^2 = 0.97$, $\%\overline{RB} = -33.8\,\%$, $\%\overline{RSD} = 27.7\,\%$ for RT-OC vs. Partisol-OC and $R^2 = 0.98$, $\%\overline{RB} = -17.9\,\%$, $\%\overline{RSD} = 18.4\,\%$ for RT-OC vs. HV-OC). The average Y/X ratios were 0.75 ± 0.11 for RT-TC vs. Partisol-TC and 0.86 ± 0.11 for RT-TC vs. HV-TC, respectively. The Y/X ratios for RT-OC vs. Partisol-OC and RT-OC vs. HV-OC were 0.72 ± 0.14 and 0.85 ± 0.18, respectively. These numbers suggest that, in general, both the TC and OC measurements from the offline filter samples were larger than those observed through the semicontinuous method. More specifically, the discrepancies were larger between RT data and Partisol data than those between RT data and HV data. In addition to the uncertainties associated with the sampling and analysis processes, another possible reason is the positive artifacts due to organic vapor adsorption on the quartz fiber filters since no denuder was used in either the Partisol or HV samplers. The amount of organic vapor adsorbed onto the quartz fiber filter in the Partisol samplers was expected to be higher than that in the HV samplers as the face velocity of the Partisol sampler is approximately half of that of the HV sampler (McDow and Huntzicker, 1990).

The EC data comparisons show a higher degree of scatter than TC and OC ($R^2 = 0.93$ for RT-EC vs. Partisol-EC and $R^2 = 0.86$ for RT-EC vs. HV-EC), while the average Y/X ratios for EC suggested that the semicontinuous data agree better with the filter-based measurements (0.88 ± 0.26 for RT vs. Partisol samples and 1.04 ± 0.38 for RT vs. HV samples, respectively). Several studies have reported poor agreement between thermal EC from the field analyzer and those filter-based EC measurements due to the high detection limit and differences in the temperature programs (e.g., Schauer et al., 2003; Bae et al., 2004; Venkatachari et al., 2006). However, the discrepancies between RT-EC and filter-based EC measured at the roadside in this study might also be attributed to the different sampling durations. The field analyzer collected $PM_{2.5}$ samples for a total of 1104 min on a daily basis, accounting for about three-quarters of the 24 h period. The air sampled by the RT-OC–EC analyzer might not be able to fully represent the 24 h integrated sampling period by the filter-based measurements because of the high carbon concentrations with large variations at MK.

3 Results and discussions

3.1 Organic and elemental carbon concentrations

The annual average OC and EC concentrations at MK AQMS during the study period were 7.8 and 4.4 $\mu g\,C\,m^{-3}$, respectively. The average OC and EC concentrations in individual months and in different seasons during the study period are shown in Fig. 2. Based on the local meteorological characteristics, the seasons were defined as follows: 16 March–15 May as spring, 16 May–15 September as summer, 16 September–15 November as fall and 16 November–15 March of the next year as winter (Chin, 1986; Yuan et al., 2006).

OC had clear seasonal variation, with higher values in the winter months (November–February) and the lowest values recorded in summertime (June–August). In comparison, EC exhibited little seasonal variation, suggesting that it dominantly came from local emission sources. The relative contributions of OC to $PM_{2.5}$ ranged from 15.5 % (July 2011) to 29.3 % (January and February 2012), while the EC percent contribution to $PM_{2.5}$ mass was the highest in summer (17.7 % in June 2011) and lowest in winter (9.2 % in December 2011). This can be explained by the quite comparable EC

concentrations throughout the year, while $PM_{2.5}$ concentrations were much lower during summertime than wintertime.

The weekly patterns showed that EC was elevated on weekdays and decreased to a minimum on Sundays for all months. OC also had the lowest values on Sundays compared to the rest of the week, but the variations were less distinct than those of EC. These patterns were consistent with the traffic flow variation within a week and confirm vehicular sources as the dominant contributor to EC and an important source of OC. For OC, unlike the EC concentrations which maintained at a stable level during the study period, its concentrations were evidently higher in winter months. If we consider relevant OC and EC measurement data in Hong Kong reported for a wider spatial coverage, the OC increment in winter (in comparison with summer) was mainly attributed to air pollutants transported into the MK area from elsewhere. A previous study examined PM_{10} EC and OC data in a monitoring network of nine general stations and the MK roadside station across Hong Kong from 1998 to 2001 (Yu et al., 2004). The winter average OC was found to be 5.7–10.5 $\mu g\,m^{-3}$ higher than the summer average OC across the monitoring network, with the highest OC seasonal increment associated with the station in the northernmost of the Hong Kong territory and the OC increment in MK (7.6 $\mu g\,m^{-3}$) similar to those recorded at a cluster of six general stations in the same airshed to the south of Tai Mo Shan (5.7–7.9 $\mu g\,m^{-3}$). Such spatial variation characteristics strongly suggest that the winter OC increment over the summer in Hong Kong was dominated by regional/super-regional sources. This is also consistent with the seasonality of prevailing background wind for Hong Kong, with northerly and northeasterly winds prevailing in winter that bring more polluted air masses from mainland China (Yu et al., 2004). Although additional local sources in winter, such as more of the semivolatile cooking emissions partitioning to the particle phase, could not be ruled out, their contributions to the winter OC increment were most likely minor in comparison with outside sources.

The diurnal variations of carbon concentrations for weekdays (Monday–Friday), Saturdays, and holidays (Sunday and public holidays) were examined for individual months (Figs. S1 and S2 in the Supplement), and 4 months were selected to represent the different seasons (Fig. 3; August for summer, October for fall, January for winter and March for spring). The EC concentrations on holidays, especially during daytime, were consistently lower in individual months, indicating on-road diesel-powered vehicles as its major sources (i.e., reduced bus schedule on holidays) and the "local" characteristics. The difference of OC concentrations between weekdays and holidays was less significant in all seasons. The potential reasons include that (1) more gasoline-powered vehicles (e.g., private cars) would offset the OC concentration reduction due to fewer diesel-powered vehicles, (2) cooking-related activities might make greater contributions during holidays, and (3) polluted air masses

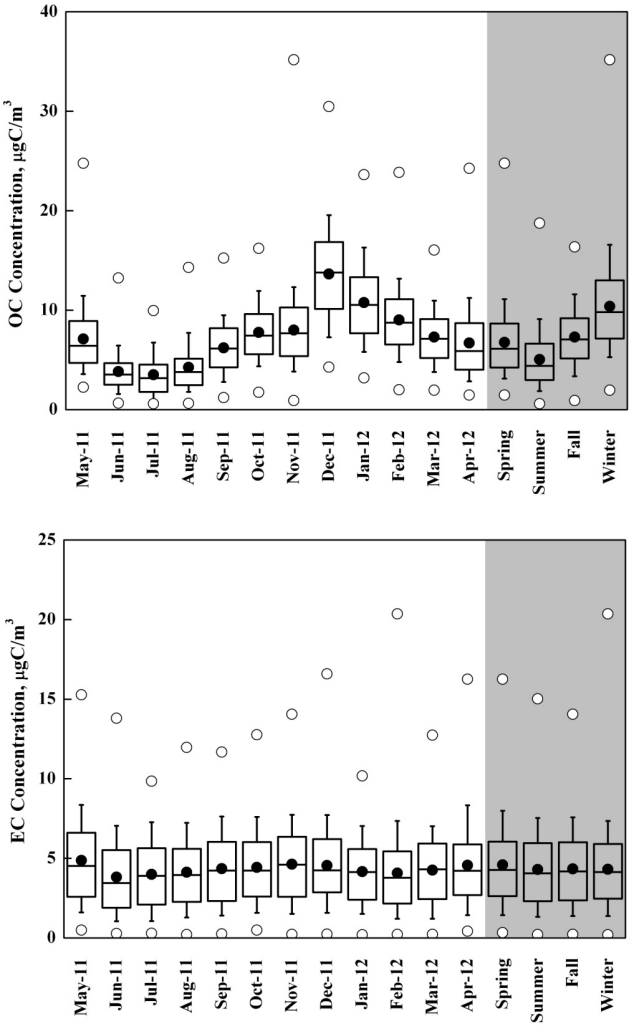

Figure 2. The 1 h OC and EC concentrations in individual sampling months and in different seasons at MK AQMS during the study period from May 2011 to April 2012 (Bottom and top of box: the 25th and the 75th percentiles; whiskers: the 10th and 90th percentiles; dot in the box: the average; line in the box: the median; white circles: the minimum and maximum values).

transported from elsewhere outside of Hong Kong make a more sizable contribution to OC, especially in winter and the two transitional seasons (Yu et al., 2004), obscuring the weekday–holiday variation in primary OC from vehicles.

The diurnal profiles for OC and EC also differ. EC concentrations started to increase from 07:00, and two peaks (07:00–11:00 and 16:00–19:00) were observed during the day. These two periods of higher EC coincided with the rush hours in the city. EC concentrations started to decrease around 19:00, and remained at a relatively low level from midnight till the next early morning. NO_x and EC were found to correlate quite well with each other, especially during the time period of 21:00–06:00. (the next day) and the first rush hour period (Fig. 4). In these two periods, the emission

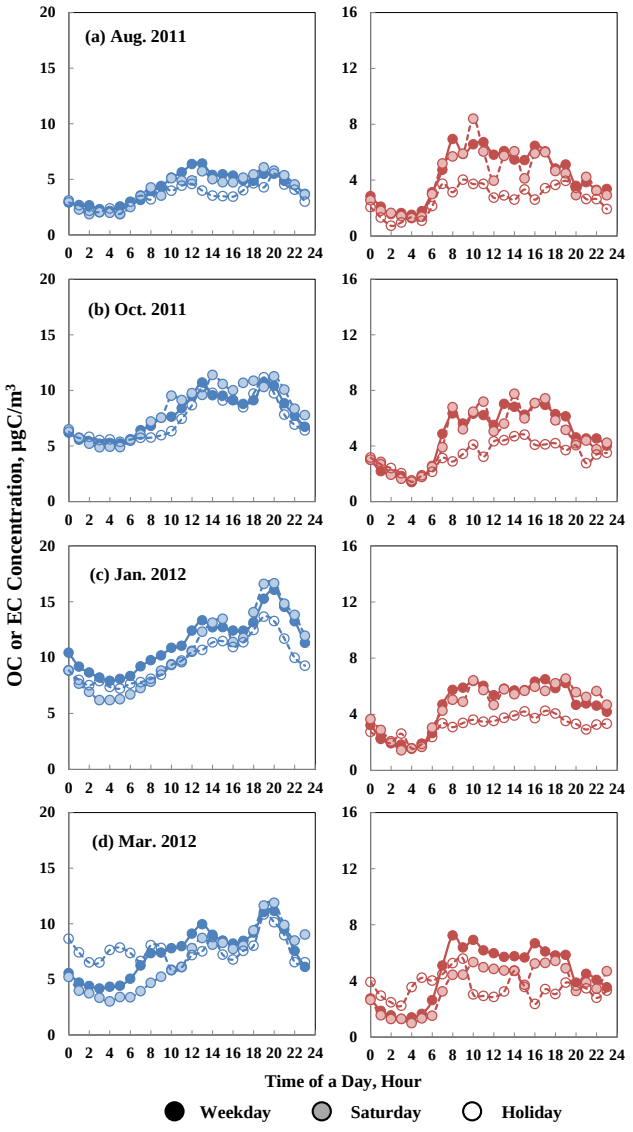

Figure 3. Diurnal variations of OC (blue dots) and EC (red dots) concentrations (unit: $\mu g\,C\,m^{-3}$) for weekdays, Saturdays and holidays at MK AQMS in **(a)** August 2011, **(b)** October 2011, **(c)** January 2012 and **(d)** March 2012.

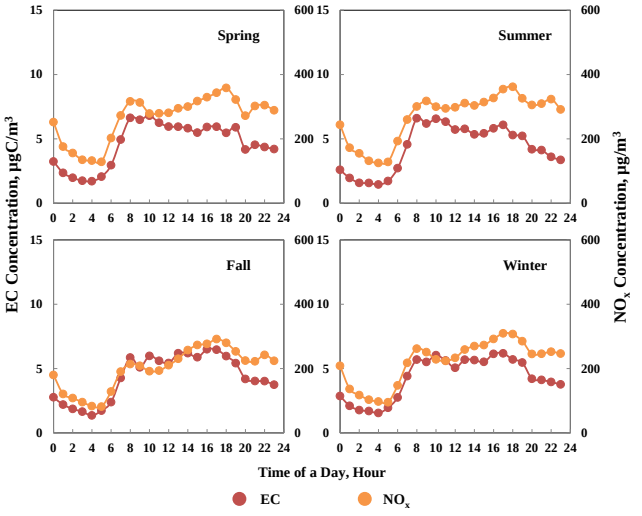

Figure 4. Diurnal variations of EC ($\mu g\,C\,m^{-3}$) and NO_x ($\mu g\,m^{-3}$) at MK AQMS during different seasons.

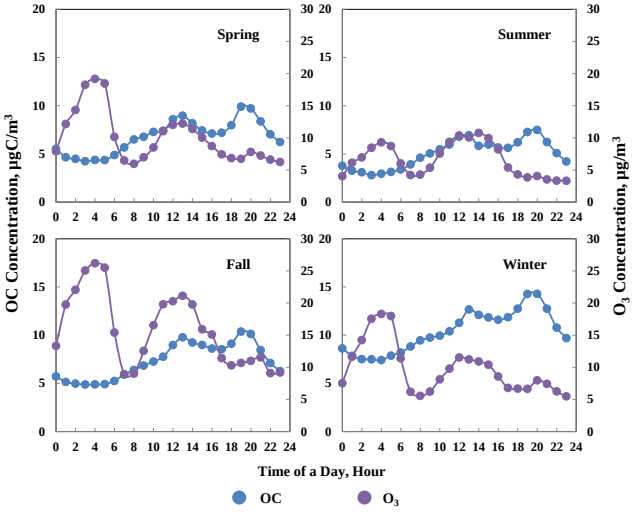

Figure 5. Diurnal variations of OC ($\mu g\,C\,m^{-3}$) and O_3 ($\mu g\,m^{-3}$) at MK AQMS during different seasons. See text for the explanation of the early morning O_3 peak.

sources at roadside were relatively limited and EC and NO_x would be primarily from vehicular exhaust. In contrast, during the rest of the day, various emission sources for NO_x, together with the higher reactivity of NO_x during daytime, could lead to a weaker correlation between NO_x and EC concentrations.

The OC concentrations also peaked twice a day (11:00–16:00 and 19:00–22:00). The diurnal profile comparison between OC and O_3 showed that one O_3 peak commonly appeared in the early afternoon but was about 1–2 h earlier than the afternoon OC peak (Fig. 5). In the roadside environment, the ozone concentration level was much lower due to titration by NO. Nevertheless, an ozone peak appearing in the early afternoon was consistently observed in different seasons (Fig. 5). Such a temporal characteristic tends to indicate that ozone could be an indicator of photochemical processes, even in a high-NO roadside environment. In view of the consistent observation of an ozone peak in the early afternoon, it is possible that the first OC peak was related to secondary organic aerosol (SOA) formation. The nighttime OC peak, on the other hand, could be associated with emissions from the larger number of mainly gasoline-fueled private cars on the road. In addition, the cooking-related activities possibly also contribute to the higher OC levels during both of the time periods. We note that there was the consistent presence of an early morning O_3 peak around 03:00–05:00 in all

months. This nighttime ozone peak is also observed across all the urban monitoring sites in Hong Kong. Integrated process analysis using chemical transport modeling (Y. Li at HKUST, personal communication, 2014) shows that vertical transport (advection and diffusion) and NO_x titration are the major processes controlling nighttime O_3 abundance in Hong Kong. The joint result of reduced NO_x titration and mixing-in of outside and upper air masses, which contain higher O_3 concentrations, is thought to account for the early morning O_3 peak that elevates to the level of background ambient air (< 20 ppb).

The different diurnal variations of OC and EC concentrations result in an OC / EC ratio pattern of three peaks appearing during the day (Fig. S3 in the Supplement). The first one is observed in the early morning, when EC concentrations were much lower than those of OC. The second peak appeared in the early afternoon, coinciding with the first OC peak. The third peak was at around 20:00, when the OC concentrations were high while EC concentrations started to decrease.

3.2 Estimation of the $(OC/EC)_{vehicle}$

The EC-tracer method, due to its simplicity, has long been used to estimate the relative contributions of primary and secondary sources to measured particulate OC (e.g., Chu and Macias, 1981; Wolff et al., 1982; Turpin et al., 1991; Turpin and Huntzicker, 1995; Cabada et al., 2004; Plaza et al., 2006; Lonati et al., 2007; Yu et al., 2009). This method is based on the assumption that EC is exclusively primary in origin and that EC and primary OC have common emission sources (e.g., combustion, resuspension of combustion particles). The measured OC concentration is the sum of POC and SOC:

$$[OC]_{measured} = POC + SOC. \quad (1)$$

POC is emitted mainly by combustion or combustion-related sources, but there might be also a minor portion from non-combustion sources (e.g., biogenic sources); therefore,

$$POC = [OC]_{combustion} + b, \quad (2)$$

where b denotes non-combustion primary OC.

If an $(OC/EC)_{pri}$ representing the primary combustion sources at the measurement site is known, POC can be calculated using the equation below:

$$POC = EC \times (OC/EC)_{pri} + b. \quad (3)$$

SOC can be subsequently derived as the difference between $[OC]_{measured}$ and POC, i.e., Eq. (4).

$$SOC = [OC]_{measured} - [EC \times (OC/EC)_{pri} + b] \quad (4)$$

Several approaches have been reported in the literature to estimate the $(OC/EC)_{pri}$, including the use of (1) emission inventories of OC and EC from primary sources (Gray et al., 1986), (2) ambient OC and EC measurements made when primary source emissions are dominant and/or when photochemical activities are weak (Turpin and Huntzicker, 1991), and (3) the minimum OC / EC ratio obtained in the study period (Lim and Turpin, 2002). It is not a trivial task to ensure that $(OC/EC)_{pri}$ determined in these approaches is representative of the composite effect of multiple primary combustion sources, each having a time-varying contribution to the ambient OC and EC. In addition, uncertainty in estimating b (see discussion later in this section) introduces additional uncertainty into the estimates of POC and SOC. While we recognize the difficulty in deriving reliable POC and SOC concentrations, by comparison we see it is a much simpler task to derive an $(OC/EC)_{vehicle}$ ratio representative of vehicular emissions for our roadside environment, since it has the unique characteristic of vehicular emissions being the dominant EC source. Once $(OC/EC)_{vehicle}$ is determined, $OC_{vehicle}$ can be calculated using Eq. (5):

$$OC_{vehicle} = EC \times (OC/EC)_{vehicle}. \quad (5)$$

The approaches we use here in estimating $(OC/EC)_{vehicle}$ are the same as the last two approaches described above for $(OC/EC)_{pri}$. We first use a subset of data that have a given percentage of the lowest OC / EC ratios among the complete data set to derive $(OC/EC)_{min}$ (Castro et al., 1999). The slope ($(OC/EC)_{min}$) and the intercept (b) in Eq. (3) were calculated via Deming regression of OC on EC using the lowest 5 % data by OC-to-EC ratio. In the Deming regression analysis, the uncertainties in both x and y axes are taken into account (Deming, 1943; Cornbleet and Gochman, 1979). Deming regression has been shown to have better performance in the EC-tracer method than the ordinary least-squares (OLS) regression, which only considers random measurement errors in y (Chu, 2005; Saylor et al., 2006).

There are different forms of Deming regression because of different ways of representing measurement errors in x and y, i.e., $\omega(X_i)$ and $\omega(Y_i)$ in Eq. (6) for S, which is the sum of the square of the perpendicular distances between the data points and the regression line (Saylor et al., 2006).

$$S = \sum[\omega(X_i)(x_i - X_i)^2 + \omega(Y_i)(y_i - Y_i)^2] \quad (6)$$

In Eq. (6), X_i and Y_i are the observed data points and x_i and y_i are the adjusted points lying on the regression line. The simplest form of Deming regression, termed default Deming regression, adopts a value of 1 for λ – the ratio of $\omega(X_i)$ and $\omega(Y_i)$ (Eq. 7). In other words, equal measurement uncertainties for variable X_i and Y_i are assumed.

$$\lambda = \omega(X_i)/\omega(Y_i) \quad (7)$$

Saylor et al. (2006) compared two forms of Deming regression, default Deming regression with $\lambda = 1$ and optimal Deming regression with an accurate representation of λ (i.e., $\lambda = \mathrm{Var}(\varepsilon_{OC})/\mathrm{Var}(\varepsilon_{EC})$, where $\mathrm{Var}(\varepsilon)$ is the variance of the

Table 1. Deming regression results of $(OC/EC)_{min}$ (the slope) and non-combustion term b (the intercept) using the lowest 5 % data by OC-to-EC ratio on a monthly, seasonal and annual basis from the 1-year carbon measurements at MK AQMS.

Time period	No. of data	λ (Y/X)[1]	$(OC/EC)_{min}$ (slope)[2]	Non-combustion term b (intercept)[2]	Correlation coefficient (R^2)
May 2011	34	0.53	0.73 (±0.025)	0.12 (±0.190)	0.83
Jun 2011	24	0.25	0.50 (±0.035)	−0.29 (±0.247)	0.64
Jul 2011	12	0.15	0.38 (±0.020)	0.18 (±0.083)	0.95
Aug 2011	24	0.27	0.52 (±0.011)	−0.24 (±0.051)	0.97
Sep 2011	36	0.29	0.54 (±0.018)	0.47 (±0.121)	0.75
Oct 2011	38	0.54	0.73 (±0.017)	0.04 (±0.097)	0.77
Nov 2011	36	0.49	0.70 (±0.032)	0.19 (±0.184)	0.44
Dec 2011	36	2.14	1.46 (±0.025)	−0.18 (±0.161)	0.90
Jan 2012	38	2.01	1.42 (±0.046)	−0.58 (±0.325)	0.70
Feb 2012	36	0.96	0.98 (±0.029)	0.25 (±0.207)	0.93
Mar 2012	34	0.62	0.78 (±0.023)	0.61 (±0.155)	0.85
Apr 2012	36	0.37	0.61 (±0.008)	0.32 (±0.048)	0.88
Summer	94	0.24	0.49 (±0.003)	−0.20 (±0.017)	0.90
Fall	72	0.45	0.67 (±0.011)	0.05 (±0.065)	0.73
Winter	142	1.02	1.01 (±0.009)	−0.23 (±0.062)	0.69
Spring	66	0.45	0.67 (±0.020)	−0.15 (±0.134)	0.63
Year	372	0.38	0.62 (±0.002)	−0.23 (±0.008)	0.80

[1] $\lambda = \mathrm{Var}(\varepsilon_{OC})/\mathrm{Var}(\varepsilon_{EC})$, where $\mathrm{Var}(\varepsilon)$ is the variance of the measurement errors, ε.
[2] Values inside parentheses are the 95 % confidence intervals.

measurement errors, ε). Using simulated EC and OC data, they demonstrated that the optimal Deming regression provides excellent results, while the default Deming regression yields a slope of 6 % larger than the true value and a negative intercept of −1.28 due to inaccurate representation of error variance. We therefore adopt optimal Deming regression in our linear regression approach to calculate $(OC/EC)_{min}$, and λ is taken to be the ratio of the measurement error variance of X and Y.

The regressions were performed on a monthly, seasonal and annual basis so as to evaluate the robustness of different subsets of data and the results are shown in Table 1. It is noted that some intercept values are negative, which does not seem to have a physical basis. To understand the issue of negative intercepts, we next examine regression lines obtained with OLS, default Deming and optimal Deming regression for the January 2012 data (Fig. S4 in the Supplement), which had the largest negative intercept (−0.58) among all the monthly $(OC/EC)_{min}$ values. The OLS regression results in a positive intercept (0.86), while the two Deming regressions give negative intercepts. The different regression lines are apparently a result of difference in assigning weights to individual observations. This result suggests that the regression line intercept is fairly sensitive to weights assigned to individual observations, or, in other words, error variances for X and Y variables. For actual ambient data, it is difficult to identify a subset of data that is free of SOC contribution, or such a subset of data simply does not exist. In addition, multiple primary combustion sources that have different $(OC/EC)_{pri}$ values coexist and their relative strengths vary with time at a given ambient location. Both factors would contribute to scattering of the data that are used for deriving $(OC/EC)_{pri}$, which in turn could lead to a negative intercept, as illustrated by Fig. S4 in the Supplement. This analysis about intercept shows the large uncertainty associated with the estimated b when using linear regression approaches. One needs to be cautious in estimating POC and SOC if a linear regression approach is relied upon for the calculation of non-combustion-derived primary OC (i.e., b in Eqs. 3 and 4). On the other hand, we note the slope is much less sensitive to different regression approaches. In the example of the January 2012 data, the slope values derived from the two Deming regressions differ less than 5 % (Fig. S4 in the Supplement). This adds to our confidence in the robustness of the derived $(OC/EC)_{min}$ using Deming regression of select ambient OC and EC data.

The monthly $(OC/EC)_{min}$ values derived using the lowest 5 % data by OC-to-EC ratio exhibited lower values during summer months. In particular, the value was 0.38 in July and 0.52 in August. Higher values of $(OC/EC)_{min}$ were observed for December 2011 (1.46) and January 2012 (1.42). The monthly variations of $(OC/EC)_{min}$ are consistent with the estimations for different seasons. The lowest value (0.49) was found in summer, which is a season mainly under the influence of local primary emissions, and from time to time the southerly winds from the ocean would bring in cleaner air to further dilute the pollution in Hong Kong. During the winter season, the prevailing winds were northerly and northeasterly

Table 2. Deming regression results of $(OC/EC)_{min}$ using subsets of summer EC and OC data varying from the lowest 5 % by OC-to-EC ratio to 100 %.

Lowest % by OC / EC	No. of data	$(OC/EC)_{min}$ (slope)[1]	Non-combustion term b (intercept)*	Correlation coefficient (R^2)
5	94	0.49 (±0.003)	−0.20 (±0.017)	0.90
10	188	0.57 (±0.003)	−0.26 (±0.013)	0.86
20	376	0.66 (±0.002)	−0.26 (±0.009)	0.78
30	564	0.76 (±0.002)	−0.38 (±0.009)	0.72
40	752	0.81 (±0.002)	−0.31 (±0.007)	0.68
50	940	0.88 (±0.001)	−0.32 (±0.007)	0.63
60	1128	0.99 (±0.002)	−0.54 (±0.007)	0.59
70	1316	1.08 (±0.002)	−0.67 (±0.007)	0.55
80	1504	1.19 (±0.002)	−0.80 (±0.007)	0.50
90	1692	1.24 (±0.002)	−0.67 (±0.007)	0.50
100	1878	1.21 (±0.002)	−0.19 (±0.006)	0.33

* Values inside parentheses are the 95 % confidence intervals.

Table 3. The average OC-to-EC ratios, calculated as ratio of average OC to average EC, in time periods of 07:00–11:00, 16:00–19:00 and 19:00–22:00 for individual months.

	Time period		
Month	07:00–11:00	16:00–19:00	19:00–22:00
May 2011	0.97	1.22	1.94
Jun 2011	0.64	0.88	1.45
Jul 2011	0.56	0.77	1.32
Aug 2011	0.70	0.82	1.29
Sep 2011	1.00	1.09	1.88
Oct 2011	1.27	1.39	2.14
Nov 2011	1.26	1.32	2.20
Dec 2011	2.36	2.45	3.66
Jan 2012	1.90	2.11	3.14
Feb 2012	1.41	1.77	3.22
Mar 2012	1.15	1.46	2.35
Apr 2012	1.04	1.20	1.76

and the regional transport of air pollutants played a significant role (Yu et al., 2004). The higher $(OC/EC)_{min}$ ratio is a combined result of primary sources having higher (OC / EC) and non-negligible contribution of SOA in the 5 % lowest (OC / EC) samples. Spring and fall are transitional seasons with prevailing winds as a combination of southerly and northerly, and therefore the $(OC/EC)_{min}$ values were recorded to be in between.

Since local primary emission sources are dominant during summertime, additional Deming regressions were performed on the summer OC and EC data set by varying the percentage of included data from the lowest 5 % to 100 % (Table 2). The regression slope gradually increases from 0.49 when the lowest 5 % data ($n = 94$) are used for regression to 1.21 as all summer data ($n = 1878$) are included for regression. The summer data and the Deming regression lines are shown in Fig. S5 in the Supplement. Based on this Deming regression analysis for this "local emissions-influenced" period, a value of 0.5 was suggested to approximate $(OC/EC)_{vehicle}$ while 1.2 could serve as an upper limit of an $(OC/EC)_{vehicle}$ estimate at this roadside site.

To evaluate the impact of different emission sources on the OC / EC ratio, we further examined the OC / EC ratios in subsets of data selected according to the carbon diurnal profiles. Three time periods were chosen, including two EC peak times (07:00–11:0 and 16:00–19:00) and one OC peak time (19:00–22:00). The appearance of EC peaks in the daytime and OC peak in the evening reflected enhancement of primary emissions during these periods. Hence, the OC / EC ratios in these time periods were more influenced by primary emissions. Table 3 lists the average OC / EC ratios, calculated as the average OC to the average EC, in the three time periods in individual months. We note that data from the identified episodic periods, defined to be periods when the hourly $PM_{2.5}$ mass concentrations exceeded the monthly average plus 1 standard deviation for 4 h or more, were excluded since on episode days the carbon concentrations were considerably influenced by more aged air masses transported from outside Hong Kong.

The average OC / EC ratio for the same time period varied with months. Higher values were observed in fall and winter months, while lower were observed in summer months (May–September). This is consistent with the hypothesis that local sources dominated in summertime while transported air masses largely impacted Hong Kong during winter, leading to higher OC / EC ratios.

Within the same month, the OC / EC ratios in the two EC peak periods were mostly comparable and 4–40 % higher in the second EC peak periods, and both periods were lower than that in the period of 19:00–22:00. This is expected since the first two periods were dominated by vehicular emissions. During these two rush hour periods of the day,

public transportation (e.g., buses, light buses, goods vehicles) were predominant on the road and most of them were diesel-powered vehicles. During the evening, more private cars, which were predominately powered by gasoline engines, were on the road. The OC / EC ratios, as reported in source profile studies, were 0.6–0.8 for diesel engine exhaust, 2.2–4.2 for catalyst-equipped gasoline exhaust, and 8.2–60.0 for noncatalyst gasoline-powered exhaust (Hildemann et al., 1991; Schauer et al., 1999a, 2002a). The compositional variation in the on-road motor vehicles is expected to result in different OC / EC ratios. The average OC / EC ratios in the 19:00–22:00 were 46–82 % higher than those in the 16:00–19:00 periods in different months. The elevation of OC relative to EC in the 19:00–22:00 could not possibly come from SOC, as the SOC contribution would be expected be higher in the 16:00–19:00 period, which was partly daytime. In view of the site in a district of numerous restaurants, the consistently higher OC / EC during 19:00–22:00 was most likely caused by cooking-related activities. Work on cooking source samples revealed that little EC was emitted from cooking, while OC accounted for 34–69 % of the emitted $PM_{2.5}$ mass (Hildemann et al., 1991; Schauer et al., 1999b, 2002b). This primary OC source from cooking would certainly increase the ambient OC / EC ratios.

The comparisons between the calculated $(OC/EC)_{min}$ values using all data versus the average OC / EC in subsets of the data under significant influence of primary emissions clearly show the difficulty in deriving a single $(OC/EC)_{pri}$ value to represent a composite of multiple primary sources, since each source makes time-varying contributions. It can also be seen that using the $(OC/EC)_{min}$ to represent the primary OC / EC ratio in the EC-tracer method would lead to overestimation of SOC during time periods when cooking-related sources were significant. Partly for this reason, we did not attempt to estimate POC and SOC in this study. On the other hand, the accumulative evidence suggests that it is reasonable to adopt a value of 0.5, the $(OC/EC)_{min}$ value derived from Deming regression of the 5 % lowest summer data by OC-to-EC ratio, to approximate the OC / EC ratio for vehicular emissions. With EC at this location being predominantly from vehicular emissions, the vehicle-related OC (i.e., $OC_{vehicle}$) is then $0.5 \times EC$. We note $OC_{vehicle}$ estimated in this way only accounts for primary OC emission from vehicles. SOC formed from volatile organic compound (VOC) precursors emitted by vehicles (e.g., toluene) is not captured in this EC-tracer approach.

3.3 Estimation of vehicle-related OC and $PM_{2.5}$

3.3.1 Estimation using $(OC/EC)_{vehicle}$ inferred from OC–EC measurements

The annual average vehicle-related OC ($OC_{vehicle}$) concentration was $2.2 \pm 1.2\,\mu g\,C\,m^{-3}$, which represents 32.0 ± 18.9 % of the annual average particulate OC. The monthly average $OC_{vehicle}$ concentrations showed little variation throughout the year ($1.9–2.4\,\mu g\,C\,m^{-3}$), while the percent contribution to total OC varied from 16.6 % in December to 64.0 % in July. By applying a ratio of 1.4 to convert OC to organic matter (OM) (Malm et al., 1994), the daily averaged contributions of vehicle-related organic aerosols ($OM_{vehicle}$) to the $PM_{2.5}$ mass were estimated to be in the range of 3.5–24.8 %. By further summing up the concentrations of $OM_{vehicle}$ and EC, the vehicle-related carbonaceous $PM_{2.5}$ ($PM_{vehicle}$) and its contributions to the $PM_{2.5}$ mass can be estimated. The monthly average $PM_{vehicle}$ ranged from 6.5 to $8.3\,\mu g\,C\,m^{-3}$ and exhibited little seasonal variation (Fig. 6), reflecting the local nature of vehicular emission source. Its relative contributions to the total $PM_{2.5}$ mass, on the other hand, varied from 16.0 % (December 2011) to 35.6 % (August 2011), with an annual average of 24.8 %. The percent contribution differences were mainly due to higher $PM_{2.5}$ levels during wintertime. Calculations also show that the average $PM_{vehicle}$ concentrations were estimated to be $10.3\,\mu g\,m^{-3}$ during the first rush hour period (07:00–11:00) on non-holidays and $6.5\,\mu g\,m^{-3}$ for the same period on holidays (including Sundays and public holidays). Hence, a reduction of approximately 37 % in $PM_{2.5}$ mass for the period of 07:00–11:00 on holidays could be attributed to reduction in vehicular emissions, which is a result of reduced on-road public transportation (e.g., diesel-powered buses). On Sundays and public holidays, bus frequencies decrease by 20–30 % compared to the rest of the week. These results indicate that the emissions from on-road vehicles are an important source of $PM_{2.5}$ in the urban roadside environment of Hong Kong.

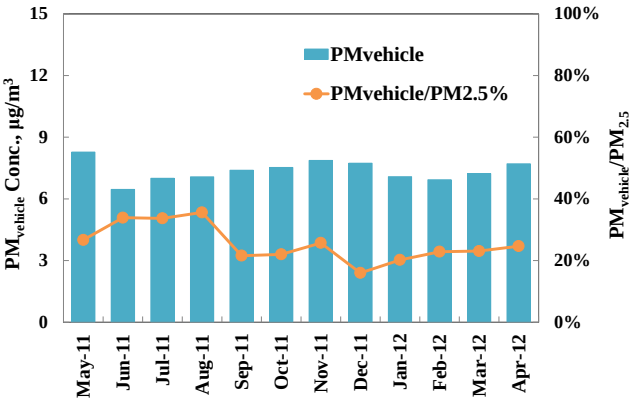

Figure 6. Monthly average vehicle-related $PM_{2.5}$ concentrations estimated by ($OM_{vehicle}$+EC) and the relative contributions to the monthly average $PM_{2.5}$ mass at MK AQMS during May 2011–April 2012. (Note: $PM_{2.5}$ mass concentrations were measured by a tapered element oscillating microbalance (TEOM 1400AB) on an hourly basis.)

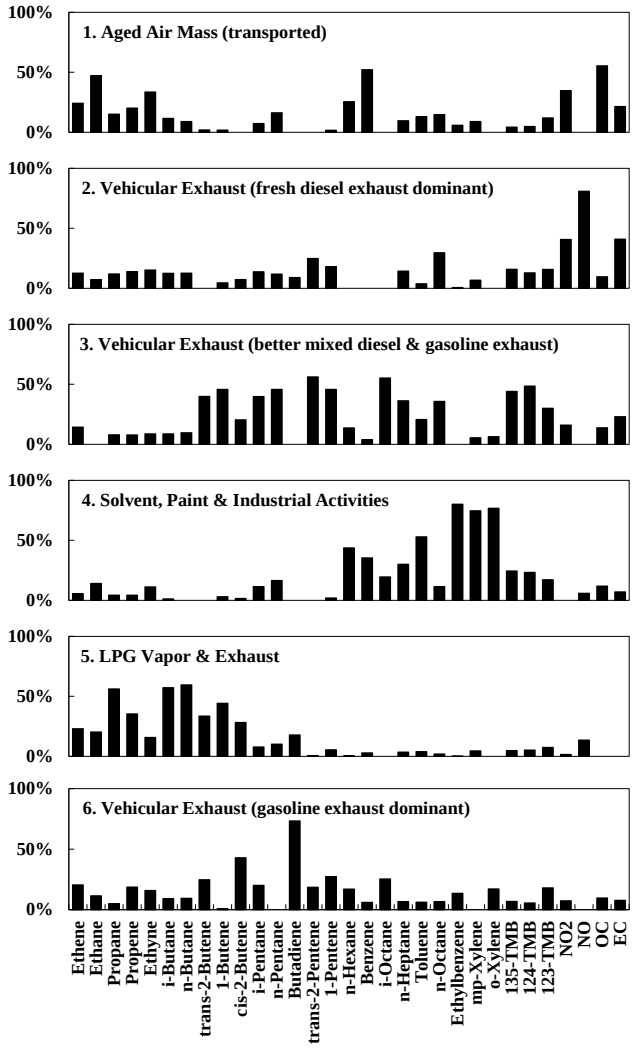

Figure 7. Source profile (% of species total) identified by USEPA PMF3.0.

3.3.2 Estimation using receptor modeling analysis

The $OC_{vehicle}$ were also estimated by means of a receptor modeling approach so that comparisons can be conducted for evaluation of the EC-tracer method. In the receptor modeling approach, source apportioning was performed on OC and EC by means of the positive matrix factorization (PMF) model. The input data consist of hourly concentrations of 27 volatile organic compounds (VOCs), NO, NO_2, OC and EC. The VOC measurements were conducted on an hourly/half-hourly basis using a GC955 series 611/811 VOC analyzer (Syntech Spectras, the Netherlands) at MK AQMS. Isoprene was excluded from the input data set since the biogenic emissions at roadside can be neglected. *iso*-Hexane was also excluded as > 30 % of its measurements were below the method detection limit.

The uncertainties for individual species were initially estimated as $(s_{ij} + \mathrm{MDL}_{ij}/3)$ (e.g., Polissar et al., 1998; Reff et al., 2007), where MDL_{ij} is the method detection limit and s_{ij} is the analytical uncertainty of the corresponding species in the data set. The analytical uncertainties were assumed to be 10 % of the species concentrations for most of the VOCs and 5 % for NO and NO_2. The smaller molecules (i.e., ethane, ethene and ethyne) coelute in the GC analysis, causing larger uncertainties. A few VOCs (e.g., 1,3,5- and 1,2,3-trimethylbenzenes, butenes and pentenes) were detected in less than 90 % of the samples. The uncertainties of these VOCs were increased by a factor of 3 in the PMF analysis. For data which are below the detection limits, the concentrations were replaced with the value $(\mathrm{MDL}_{ij}/2)$ and the corresponding uncertainty was set to $((5/6) \times \mathrm{MDL}_{ij})$ (Polissar et al., 1998).

The source apportioning modeling was performed using EPA PMF 3.0 software (available at http://www.epa.gov/heasd/research/pmf.html). This software provides the bootstrap model, which is based on the Monte Carlo principle to check the mathematical stability of selected runs (Norris et al., 2008). Each modeling run included 20 base runs, and the base run with the minimum Q value was retained as the solution. Solutions for 4–9 factors were tested and the six-factor solution was considered to be the reasonable one. The source profiles of the six-factor solution are shown in Fig. 7.

The first factor is rich in ethane, ethyne and benzene, all of which are relatively stable species. This factor is therefore associated with an aged air mass, which was transported from other places. During the aging processes, reactive compounds such as alkenes would decay more rapidly than unreactive species and the oxidative state of the aerosols would be increased. The OC / EC ratio in this source profile was higher than 2, consistent with the nature of aged air masses.

The second, third and sixth factors are all identified as vehicular emissions from diesel-powered and gasoline-powered engines. The second factor is proposed to be dominated by diesel exhaust as it is characterized by the presence of 1,3,5-trimethylbenzene, 1,2,4-trimethylbenzene and 1,2,3-trimethylbenzene. The three VOC species appear in the distinct source profile of Hong Kong diesel fuel, as reported by Tsai et al. (2006). In particular, this factor is associated with the lowest OC / EC ratio (0.44) among all the factors, together with a large amount of NO. These characteristics strongly suggest the association of this factor with freshly emitted diesel exhaust. The third factor is dominated by *i*-pentane, *n*-pentane, pentenes and three trimethylbenzenes. Since pentanes have been reported as markers of gasoline vapors in Hong Kong (Tsai et al., 2006) and the OC / EC ratio in this factor (1.13) is higher than that in the second factor, it is suggested that the third factor represents the better mixed air mass. The sixth factor is related to gasoline-powered engine exhaust, characterized by the presence of *i*-pentane, which is the major component in gasoline vapor, and *cis*-2-butene and 1,3-butadiene, which are two common indicators for vehicle

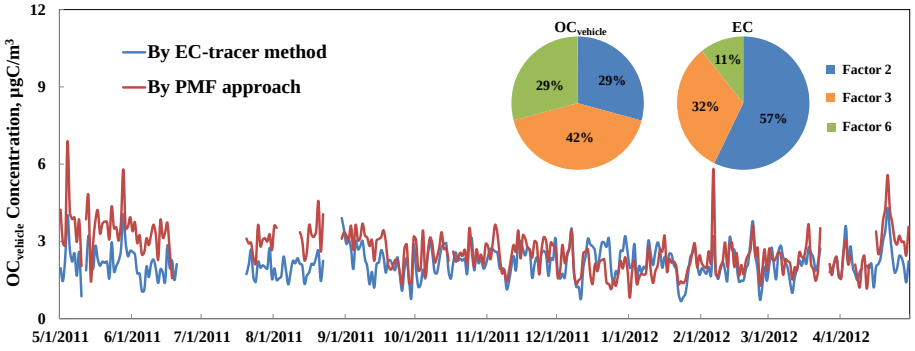

Figure 8. Time-series daily averaged $OC_{vehicle}$ ($\mu g\,C\,m^{-3}$) estimated by means of the EC-tracer method (blue curve) and the PMF approach (red curve) at MK AQMS during May 2011–April 2012. The relative contributions of different vehicular emission-related factors to the $OC_{vehicle}$ and EC, estimated by means of PMF, are shown in the pie charts.

exhaust. The OC / EC ratio in this factor (2.36) is higher than that in the other two factors.

The fourth factor is distinguished by a large amount of toluene, benzene, ethylbenzene, xylenes, and C_6 and C_7 alkanes. This source is considered to be a composite of emissions from solvent use, architectural paints and industrial activities (Seila et al., 2001; Chan et al., 2006). The industrial and architectural sources are an important source of aromatic VOCs, but they make limited contributions to particulate OC and EC at MK.

The fifth factor is dominated by propane, *i*-butane and *n*-butane, and hence is identified as the emissions from the use of liquefied petroleum gas (LPG) in vehicles, gas stations and cooking activities (Blake and Rowland, 1995). It is noted that LPG combustion and vapors barely contributed to the carbon fraction in $PM_{2.5}$ since the light alkanes emitted from LPG are too volatile to reside in the particle phase.

On the basis of the source identifications, OC apportioned into the second, third, fifth and sixth factors were summed up to represent the PMF-derived $OC_{vehicle}$. The comparison of daily $OC_{vehicle}$ obtained from the EC-tracer method and the PMF approach is shown in a time series plot (Fig. 8). A fairly good agreement was observed between the estimations from the two methods ($R^2 = 0.96$). On average, PMF-derived $OC_{vehicle}$ values were approximately 25 % higher than those calculated by means of the EC-tracer method. The discrepancies could be due to one or a combination of the following reasons: (1) uncertainties in the PMF analysis, (2) uncertainty in the $(OC / EC)_{vehicle}$ caused by the variation of the vehicle composition and (3) omission of the cooking-related OC.

The relative contributions of different vehicular emission sources to the $OC_{vehicle}$ and EC were estimated via the PMF approach (Fig. 8, pie charts). The diesel-dominant factor (Factor 2) contributed the most to EC and approximately one-third to $OC_{vehicle}$. The gasoline-dominant factor (Factor 6) contributed the least to EC but the most to $OC_{vehicle}$. These estimations indicate that both diesel-powered and gasoline-powered vehicles are significant contributing sources to the carbonaceous particle levels at the roadside.

4 Conclusions

$PM_{2.5}$ carbon measurements of hourly time resolution were conducted for the first time in a roadside environment of Hong Kong over a 12-month period from May 2011 to April 2012. Three levels of validation were performed, and the data valid rate for the entire sampling period is approximately 96 %. The OC and EC concentrations at MK AQMS during the study period were on average 7.8 and 4.4 $\mu g\,C\,m^{-3}$, respectively. Higher OC concentrations were recorded during winter months as a result of the contributions of regional air pollutant transport. EC concentrations were comparable among individual months. In addition, the EC concentrations peaked in two time periods which coincided with the traffic rush hours of a day. Both results indicate that EC was dominantly emitted from local vehicular sources.

The minimum OC / EC ratios for periods of elevated EC were derived using Deming regression. The results indicated that using a single value to represent $(OC / EC)_{pri}$ for the purpose of estimating POC and SOC by the EC-tracer method may cause significant biases since there were multiple significant primary emission sources in the sampling area, each making time-varying contributions. On the other hand, a value of 0.5, mainly based on OC and EC measurements in the lowest 5 % by OC-to-EC ratio in the summer during which local emissions dominated as a result of prevailing meteorological conditions, can be proposed to reasonably approximate the OC / EC ratio for primary vehicular emissions. The annual average vehicle-related OC concentration was subsequently estimated to be $2.2 \pm 1.2\,\mu g\,C\,m^{-3}$, which accounted for 32.0 ± 18.9 % of the total $PM_{2.5}$ OC. The monthly average $OC_{vehicle}$ concentrations had a small variation throughout the year (1.9–2.4 $\mu g\,C\,m^{-3}$), while its contribution to total OC varied from 16.6 % (December 2011)

to 64.0 % (July 2011). The $OC_{vehicle}$ derived from source apportionment analysis by PMF are in good agreement with the estimates using the proposed $(OC/EC)_{vehicle}$, adding confidence to the estimated primary OC contribution from the vehicular source. Assuming an OM-to-OC ratio of 1.4, the daily averaged contributions of $OM_{vehicle}$ to $PM_{2.5}$ ranged from 3.5 to 24.8 %. The annual average concentration of $PM_{vehicle}$ was estimated to be 7.4 $\mu g\,m^{-3}$ and accounted for approximately 25 % of the $PM_{2.5}$ concentration, confirming vehicular emissions as an important source of $PM_{2.5}$ mass.

The carbon diurnal profiles also suggest cooking-related activities as an important primary source to OC in the study area, making it difficult to rely on the EC-tracer method to estimate the relative contributions of POC and SOC. Higher resolution measurements of particle-phase tracer compounds for the cooking sources (e.g., C_{16} and C_{18} fatty acids) and for the vehicle-related SOA (e.g., phthalic acid) in conjunction with receptor modeling could provide possibilities for a more accurate estimation of SOA contributions in the urban areas of Hong Kong.

The Supplement related to this article is available online at doi:10.5194/acp-14-9279-2014-supplement.

Acknowledgements. This work is supported by the Hong Kong Environmental Protection Department (HKEPD) (tender ref. AS 10-336) and the Environment and Conservation Fund/Woo Wheelock Green Fund (ECWW09EG04). We thank HKEPD for provision of the real-time $PM_{2.5}$ and VOC data sets. Special thanks go to Damgy H. L. Chan of HKEPD for her many inputs, her tireless efforts in gathering a voluminous amount of the real-time VOC data, and assistance in sampling logistics. The content of this paper does not necessarily reflect the views and policies of the HKSAR Government, nor does mention of trade names or commercial products constitute an endorsement or recommendation of their use.

Edited by: N. L. Ng

References

Bae, M. S., Schauer, J. J., DeMinter, J. T., Tunner, J. R., Smith, D., and Cary, R. A.: Validation of a semi-continuous instrument for elemental carbon and organic carbon using a thermal-optical method, Atmos. Environ., 38, 2885–2893, 2004.

Birch, M. E. and Cary, R. A.: Elemental carbon-based method for monitoring occupational exposures to particulate diesel exhaust, Aerosol Sci. Technol., 25, 221–241, 1996.

Blake, D. R. and Rowland F. S.: Urban leakage of liquefied petroleum gas and its impact on Mexico City air quality, Science, 269, 953–956, 1995.

Cabada, J. C., Pandis, S. N., Subramanian, R., Robinson, A. L., Polidori, A., and Turpin, B.: Estimating the secondary organic aerosol contribution to $PM_{2.5}$ using the EC tracer method, Aerosol Sci. Technol., 38, 140–155, 2004.

Castro, L. M., Pio, C. A., Harrison, R. M., and Smith, D. J. T.: Carbonaceous aerosol in urban and rural European atmospheres: estimation of secondary organic carbon concentrations, Atmos. Environ., 33, 2771–2781, 1999.

Chan, L. Y., Chu, K. W., Zou, S. C., Chan, C. Y., Wang, X. M., Barletta, B., Blake, D. R., Guo, H., and Tsai, W. Y.: Characteristics of nonmethane hydrocarbons (NMHCs) in industrial, industrial-urban, and industrial-suburban atmospheres of the Pearl River Delta (PRD) region of South China, J. Geophys. Res., 111, D11304, doi:10.1029/2005JD006481, 2006.

Chin, P. C.: Climate and weather, A Geography of Hong Kong, edited by: Chiu, T. N. and So, C. L., Oxford University Press, New York, 69–85, 1986.

Chu, L. C. and Macias, E. S.: Carbonaceous urban aerosol – primary or secondary?, in Atmospheric Aerosol Source Air Quality Relationships, edited by: Macias, E. S. and Hopke, P. K., 251–268, 1981.

Chu, S.-H: Stable estimate of primary OC / EC ratio in the EC tracer method, Atmos. Environ., 39, 1383–1392, 2005.

Cornbleet, P. J. and Gochman, N.: Incorrect least-squares regression coefficients, Clin. Chem., 25, 432–438, 1979.

Deming, W. E.: Statistical adjustment of data, Wiley, NY, USA, 1943.

DRI (Desert Research Institute): Measurements and validation for 2008 / 2009 particulate matter study in Hong Kong, 2010, $PM_{2.5}$ speciation study in Hong Kong, available at: http://www.epd.gov.hk/epd/english/environmentinhk/air/studyrpts/files/HKEPDFinalReportRev_11-29-10_v2.pdf, last access: 30 August 2014, 2010.

Gelencsér, A.: Carbonaceous Aerosol, Springer, the Netherlands, 2004.

Gray, H. A., Cass, G. R., Huntzicker, J. J., Heyerdahl, E. K., and Rau, J. A.: Characteristics of atmospheric organic and elemental carbon particle concentrations in Los-Angeles, Environ. Sci. Technol., 20, 580–589, 1986.

Guo, H., Ding, A. J., So, K. L., Ayoko, G., Li, Y. S., and Hung, W. T.: Receptor modeling of source apportionment of Hong Kong aerosols and the implication of urban and regional contribution, Atmos. Environ., 43, 1159–1169, 2009.

Hildemann, L. M., Markowski, G. R., and Cass, G. R.: Chemical composition of emissions from urban sources of fine organic aerosol, Environ. Sci. Technol., 25, 744–759, 1991.

Hu, D., Bian, Q., Lau, A. K. H., and Yu, J. Z.: Source apportioning of primary and secondary organic carbon in summer $PM_{2.5}$ in Hong Kong using positive matrix factorization of secondary and primary organic tracer data, J. Geophys. Res., 115, D16204, doi:10.1029/2009JD012498, 2010.

HKEPD (Environmental Protection Department, the Government of the HKSAR): Hong Kong's Environment, available at: http://www.epd.gov.hk/epd/english/environmentinhk/air/air_maincontent.html, last access: 30 August 2014, 2013.

HKUST (the Hong Kong University of Science & Technology): Measurements and validation for the twelve-month particulate matter study in Hong Kong, 2012, $PM_{2.5}$ speciation study in Hong Kong, available at: http://www.epd.gov.hk/epd/english/environmentinhk/air/studyrpts/files/final_report_mvtmpms_2012.pdf, last access: 30 August 2014, 2013.

IARC (International Agency for Research on Cancer): IARC monographs on the evaluation of carcinogenic risks to humans, volume 105: Diesel and gasoline engine exhausts and some nitroarenes, World Health Organization (WHO), United Nations (UN), available at: http://www.iarc.fr/en/media-centre/pr/2012/pdfs/pr213_E.pdf, last access: 30 August 2014, 2012.

IPCC (Intergovernmental Panel on Climate Change): Climate Change 2007 (AR4): The Physical Science Basis, Cambridge University Press, UK, 2007.

Kang, C.-M., Koutrakis, P., and Suh, H. H.: Hourly measurements of fine particulate sulfate and carbon aerosols at the Harvard-U.S. Environmental Protection Agency Supersite in Boston, J. Air Waste Manag. Assoc., 60, 1327–1334, 2010.

Lim, H. J. and Turpin, B. J.: Origins of primary and secondary organic aerosol in Atlanta: results of time-resolved measurements during the Atlanta supersite experiment, Environ. Sci. Technol., 36, 4489–4496, 2002.

Lonati, G., Ozgen, S., and Giugliano, M.: Primary and secondary carbonaceous species in $PM_{2.5}$ samples in Milan (Italy), Atmos. Environ., 41, 4599–4610, 2007.

Malm, W. C., Sisler, J. F., Huffman, D., Eldred, R. A., and Cahill, T. A.: Spatial and seasonal trends in particle concentration and optical extinction in the United States, J. Geophys. Res., 99, 1347–1370, 1994.

McDow, S. R. and Huntzicker, J. J.: Vapor adsorption artifact in the sampling of organic aerosol: face velocity effects, Atmos. Environ., 24A, 2563–2571, 1990.

NIOSH: Monitoring of diesel particulate exhaust in the workplace, Third supplement to Manual of Analytical Methods, 4th Edition, Cincinnati, OH. Publication No. 2003–154, 2003.

Norris, G., Vedantham, R., Wade, K., Brown, S., Prouty, J., Foley, C., and Martin, L.: EPA Positive Matrix Factorization (PMF) 3.0 Fundamentals & User Guide, US Environmental Protection Agency, 2008.

Ogren, J. A. and Charlson, R. J.: Elemental carbon in the atmosphere: cycle and lifetime, Tellus, 35B, 241–254, 1983.

Plaza, J., Gómez-Moreno, F. J., Núñez, L., Pujadas, M., and Artíñano, B.: Estimation of secondary organic aerosol formation from semi-continuous OC-EC measurements in a Madrid suburban area, Atmos. Environ., 40, 1134–1147, 2006.

Polidori, A., Turpin, B. J., Lim, H.-J., Cabada, J. C., Subramanian, R., Pandis, S. N., and Robinson, A. L.: Local and regional secondary organic aerosol: insights from a year of semi-continuous carbon measurements at Pittsburgh, Aerosol Sci. Technol., 40, 861–872, 2006.

Polissar, A. V., Hopke, P. K., Zhou, L., Paatero, P., Park, S. S., and Ondov, J. M.: Atmospheric aerosol over Alaska 2. elemental composition and sources, J. Geophys. Res., 103, 19045–19057, 1998.

Reff, A., Eberly, S. I., and Bhave, P. V.: Receptor modeling of ambient particulate matter data using Positive Matrix Factorization: review of existing methods, J. Air Waste Manage. Assoc., 57, 146–154, 2007.

Saylor, R. D., Edgerton, E. S., and Hartsell, B. E.: Linear regression techniques for use in the EC tracer method of secondary organic aerosol estimation, Atmos. Environ., 40, 7546–7556, 2006.

Schauer, J. J., Kleeman, M. J., Cass, G. R., and Simoneit, B. R. T.: Measurement of emissions from air pollution sources. 2. C_1 through C_{30} organic compounds from medium duty diesel trucks, Environ. Sci. Technol., 33, 1578–1587, 1999a.

Schauer, J. J., Kleeman, M. J., Cass, G. R., and Simoneit, B. R. T.: Measurement of emissions from air pollution sources. 1. C_1 through C_{29} organic compounds from meat charbroiling, Environ. Sci. Technol., 33, 1566–1577, 1999b.

Schauer, J. J., Kleeman, M. J., Cass, G. R., and Simoneit, B. R. T.: Measurement of emissions from air pollution sources. 5. C_1–C_{32} organic compounds from gasoline-powered motor vehicles, Environ. Sci. Technol., 36, 1169–1180, 2002a.

Schauer, J. J., Kleeman, M. J., Cass, G. R., and Simoneit, B. R. T.: Measurement of emissions from air pollution sources. 4. C_1–C_{27} organic compounds from cooking with seed oils, Environ. Sci. Technol., 36, 567–575, 2002b.

Schauer, J. J., Mader, B. T., DeMinter, J. T., Geidemann, G., Bae, M. S., Seinfeld, J. H., Flagan, R. C., Cary, R. A.,Smith, D. , Huebert, B. J., Bertram, T., Howell, S., Kline, J. T., Quinn, P., Bates, T., Turpin, B., Lim, H. J., Yu, J. Z., Yang, H., and Keywood, M. D.: ACE-Asia intercomparison of a thermal-optical method for the determination of particle-phase organic and elemental carbon, Environ. Sci. Technol., 37, 993–1001, 2003.

Seila, R. L., Main, H. H., Arriaga, J. L., Martinez, G. V., and Ramadan, A. B.: Atmospheric volatile organic compounds measurements during the 1996 Paso del Norte ozone study, Sci. Total Environ., 276, 153–169, 2001.

Seinfeld, J. H. and Pandis, S.: Atmospheric Chemistry and Physics: From Air Pollution to Climate Change, Wiley, New York, USA, 1998.

Tsai, W. Y., Chan, L. Y., Blake, D. R., and Chu, K. W.: Vehicular fuel composition and atmospheric emissions in South China: Hong Kong, Macau, Guangzhou, and Zhuhai, Atmos. Chem. Phys., 6, 3281–3288, doi:10.5194/acp-6-3281-2006, 2006.

Turpin, B. J., Cary, R. A., and Huntzicker, J. J.: An in-situ, time-resolved analyzer for aerosol organic and elemental carbon, Aerosol Sci. Technol., 12, 161–171, 1990.

Turpin, B. J. and Huntzicker, J. J.: Secondary formation of organic aerosol in the Los-Angeles Basin – a descriptive analysis of organic and elemental carbon concentrations, Atmos. Environ. Part A General Topics, 25, 207–215, 1991.

Turpin, B. J., Huntzicker, J. J., Larson, S. M., and Cass, G. R.: Los Angeles mid-day particulate carbon: primary and secondary aerosol, Environ. Sci. Technol., 25, 1788–1793, 1991.

Turpin, B. J., Huntzicker, J. J., and Hering, S. V.: Investigation of organic aerosol sampling artifacts in the Los Angeles basin, Atmos. Environ., 28, 3061–3071, 1994.

Turpin, B. J. and Huntzicker, J. J.: Identification of secondary organic aerosol episodes and quantitation of primary and secondary organic aerosol concentrations during SCAQS, Atmos. Environ., 29, 3527–2544, 1995.

USEPA (Environmental Protection Agency, USA): Health assessment document for diesel engine exhaust, Office of Research and Development, Research Triangle Park, NC, available at: http://www.epa.gov/ttn/atw/dieselfinal.pdf, last access: 30 August 2014, 2002.

USEPA (Environmental Protection Agency, USA): Air quality criteria for particulate matter, volumes 1 & 2, Office of Research and Development, Research Triangle Park, NC, 2004.

Venkatachari, P., Zhou, L., Hopke, P. K., Schwab, J. J., Demerjian, K. L., Weimer, S., Hogrefe, O., Felton, D., and Rattigan,

O.: An intercomparison of measurement methods for carbonaceous aerosol in the ambient air in New York City, Aerosol Sci. Technol., 40, 788–795, 2006.

Wolff, G. T., Groblicki, P. J., Cadle, S. H., and Countess, R. J.: Particulate carbon at various locations in the United States, in: Particulate Carbon: Atmospheric Life Cycle, edited by: Wolff, G. T. and Klimisch, R. L., Plenum, New York, 297–315, 1982.

Wu, C., Ng, W. M., Huang, J. X., Wu, D., and Yu, J. Z.: Determination of elemental and organic carbon in $PM_{2.5}$ in the Pearl River Delta region: inter-instrument (Sunset vs. DRI Model 2011 thermal/optical carbon analyzer) and inter-protocol comparisons (IMPROVE vs. ACE-Asia protocol), Aerosol Sci. Technol., 46, 610–621, 2012.

Yu, J. Z., Tung, J. W. T., Wu, A. W. M., Lau, A. K. H., Louie, P. K. K., and Fung, J. C. H.: Abundance and seasonal characteristics of elemental and organic carbon in Hong Kong PM_{10}, Atmos. Environ., 38, 1511–1521, 2004.

Yu, X.-Y., Cary, R. A., and Laulainen, N. S.: Primary and secondary organic carbon downwind of Mexico City, Atmos. Chem. Phys., 9, 6793–6814, doi:10.5194/acp-9-6793-2009, 2009.

Yuan, Z. B., Yu, J. Z., Lau, A. K. H., Louie, P. K. K., and Fung, J. C. H.: Application of positive matrix factorization in estimating aerosol secondary organic carbon in Hong Kong and its relationship with secondary sulfate, Atmos. Chem. Phys., 6, 25–34, doi:10.5194/acp-6-25-2006, 2006.

Zheng, M., Hagler, G. S. W., Ke, L., Bergin, M. H., Wang, F., Louie, P. K. K., Salmon, L., Sin, D. W. M., Yu, J. Z., and Schauer, J. J.: Composition and sources of carbonaceous aerosols at three contrasting sites in Hong Kong, J. Geophys. Res., 111, D20313, doi:10.1029/2006JD007074, 2006.